



# Numerical Experimental Study on Fracture Extension Law of Hydraulic Fracturing Based on Particle Discrete Element

Jiangchun Hu<sup>1</sup>, Miao Liu<sup>1\*</sup>, Luyang An<sup>2</sup>, Bing Liu<sup>1</sup>, Mengyuan Li<sup>1</sup>

<sup>1</sup>School of Architecture and Civil Engineering, Zhongyuan University of Technology, Zhengzhou 450007, China

<sup>2</sup>Xinjiang North Construction Group Co. Ltd, Xinjiang 830063, China

\*Corresponding author's e-mail: 1366033152@qq.com

**Abstract.** The research of hydraulic fracturing theory and technology is developed with the development of oil and natural gas, and in the petroleum industry, hydraulic fracturing technology has been an important measure to increase the production of oil and natural gas. In order to study the crack extension law of rock body by hydraulic fracturing, sandstone is taken as the research object, and a hydraulic fracturing model is established on the basis of Cundall's fluid-solid coupling theory to analyze the rupture as well as the crack extension of hydraulic fracturing under different influencing factors. The results show that hydraulic fracturing cracks expand along the direction of the maximum principal stress, and when the horizontal principal stress is equal to the vertical principal stress, the direction of crack expansion is not fixed. As the ground stress field increases, the hydraulic fracture rupture pressure of the rock gradually increases; as the diameter of the well bore increases, the rock fracture pressure decreases. The results can provide some reference for a better understanding of model initiation and crack extension.

**Keywords:** Hydraulic fracturing; Fracture extension; Discrete unit method

## 1 Introduction

The fracture morphology of hydraulic fracturing is the core index for evaluating the fracturing effect [1-2], and its extension mechanism is controlled by the complexity of water-rock coupling. Existing studies have revealed the macroscopic laws through in-house experiments and numerical simulations: Jiang Yulong and Zhang Tongjing et al [3-4] found that the grouting rate dominates the fracture initiation pressure and time, but the physical tests are limited by the means of monitoring, which makes it difficult to analyse the dynamic evolution of microfractures. Huang Bingxiang et al [5-7] demonstrated that the perimeter pressure principal stress difference controlled the crack direction through indoor tests, however, such studies could not simulate the competitive

extension of multiple cracks. Finite element methods (e.g., the Papanastasio fully coupled model [8] and Li Lianchong's RFPA simulations [9-10]) can predict crack morphology, but their mesh dependence and limitations in pre-determined crack paths make it difficult to characterise the self-organised rupture behaviour of discontinuous media. These results indicate that there are significant gaps in the existing methods in revealing micro-scale fluid-particle interactions and multi-fracture dynamic competition mechanisms, both of which are key challenges in optimising fracture design and fracture network prediction.

To address the above problems, this paper innovatively adopts the Cundall fluid-solid coupling algorithm to construct a refined model of sandstone hydraulic fracturing on the PFC2D discrete element platform. Compared with the traditional method, this numerical method can accurately reproduce the whole process of microfracture emergence and competitive extension of multi-branch fractures through explicit simulation of inter-particle bonding rupture. By systematically designing the control variables of ground stress ratio and initial porosity, we focus on the nonlinear relationship between fracture initiation pressure, expansion path and stress state, and reveal the regulation of pore structure on the coupling mechanism of fluid seepage-fracture expansion. The results of the study not only provide theoretical basis for the fracture-oriented control in deep shale gas development, but also focus on the coupled modelling of 3D geological formations and natural fracture networks in subsequent studies.

## 2 Hydraulic Fracturing Rock Modeling

### 2.1 Model Building

The first step in using a PFC program to simulate and analyze the mechanical behavior of a material is to create an initial model, in order to make the numerical simulation results can truly and effectively reflect the actual physical process, the establishment of the model needs to meet the following conditions:

- For geotechnical materials, which are composed of fine particles, the size of the particles in the model should be as close as possible to the simulated object, taking into account the computational capability of the computer and the workload, the particle size distribution of the model should meet the specified requirements and correspond to the particle size distribution of the simulated object.
- The amount of overlap between neighboring particles in the initial model should be as small as possible.
- The particles in the initial model should be in force equilibrium - the combined force on each particle should be equal to 0.

This paper establishes a numerical model for hydraulic fracturing of rocks by taking sandstone as the research object, as shown in Figure 1. The rock model is 150mm long and 150mm wide, the particles are modeled with parallel adhesive contacts, and the particle radii follow a uniform distribution between the largest and smallest radii, The minimum radius is 1/80th of the model's side length, and the ratio of the maximum to

minimum radius is 1.66. Velocity is applied to the model to obtain the vertical principal stress  $\sigma_V$  and the horizontal principal stress  $\sigma_H$ , the injection wellbore for the fracturing fluid was created in the center of the rock model, and the model fine view parameters are shown in Table 1.

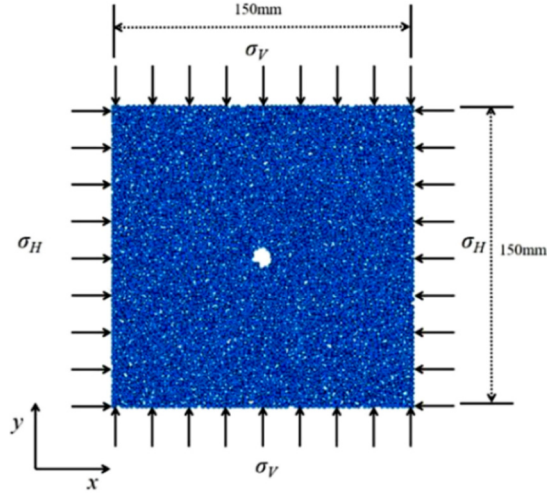


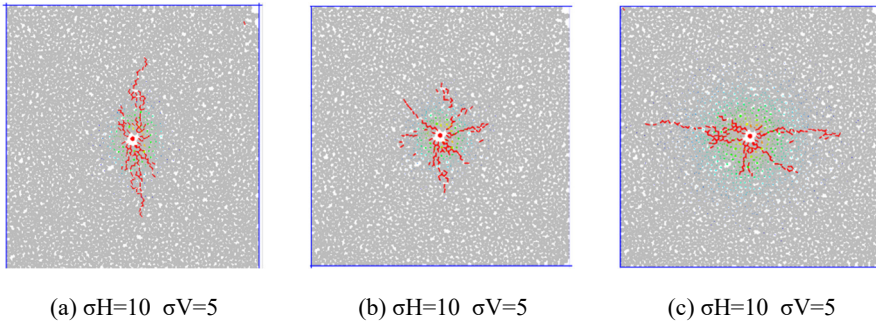
Fig. 1. Diagram of hydraulic fracturing rock models.

Table 1. Fine-scale parameters of the parallel bonding model.

Emod/GPa	kra	pb_emod/GPa	pb_emod/GPa	pb_coh/MPa	pb_ten/MPa	pb_fa/°	fric
2.89	1.5	2.89	1.5	20.941	16.608	60.25	0.5

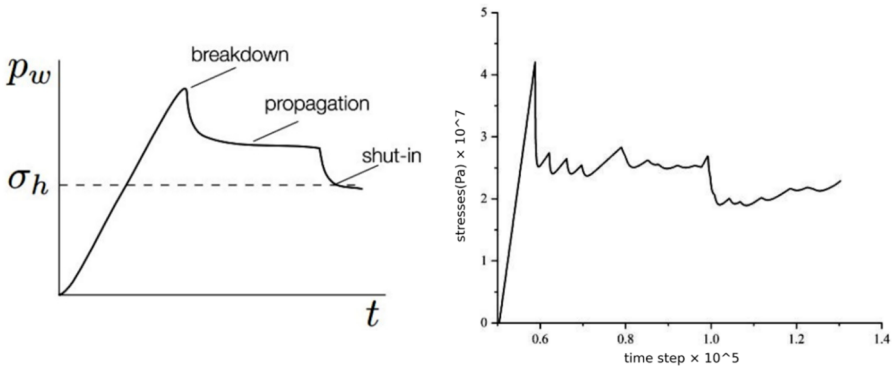
## 2.2 Validation of Numerical Simulations

In this paper, based on the principle of Cundall fluid-solid coupling, we refer to the related literature[12-13] to write the numerical simulation algorithm of hydraulic fracturing for PFC2D5.0 program, and we also need to validate the written Fish function before conducting the experiments. The ground stress ratio was set to be 2:1, 1:1, and 1:1.5, respectively, based on the model described in the previous section. Based on the servo mechanism, the same vertical stress of 10 MPa and different horizontal principal stresses of 5 MPa, 10 MPa, and 15 MPa are applied to the model. As shown in Figure 2 for the crack extension results, as can be seen from the figure, the horizontal principal stresses are different from the vertical principal stresses, cracks expand in the direction of the maximum principal stress, respectively, and when the horizontal principal stress is equal to the vertical principal stress, the direction of crack expansion is not fixed, the crack angle is basically a 120°. The cracking results are in general agreement with the theoretical results [14].



**Fig. 2.** Hydraulic fracturing fracture extension result map.

As shown in Figure 3, the pressure curve of hydraulic fracturing of rock is shown, in which (a) is the theoretical pressure curve, which represents three different stages in the process of hydraulic fracturing of rock: elastic deformation, tensile damage, and stable expansion. The pressure in the wellbore firstly increases linearly and continuously, then destruction occurs and the pressure decreases abruptly, and finally the fracture expands stably and the pressure is basically unchanged. In the above theoretical pressure curve, the rock initiation pressure is equal to the fracture pressure equal to the peak pressure in the curve. As shown in Figure (b), the variation curve of experimental pressure with time step for numerical simulation at  $\sigma_V=10$  and  $\sigma_H=10$ . Compared with Figure (a), the numerical simulation experimental pressure curve has a certain error with the theoretical pressure graph, which is due to the permeability and the seepage effect of the fracturing fluid on the pressure. However, as a whole, they are basically the same, with the same stages of growth before rock rupture, rapid decline after fracture initiation and stable expansion of the fracture.



(a) Theoretical pressure curve for hydraulic fracturing [15]. (b) Variation curve of hydraulic fracturing pressure with  $\sigma_V=10$  and  $\sigma_H=10$ .

**Fig. 3.** Hydraulic fracturing pressure curve.

### 3 Research on the Influencing Factors of Hydraulic Fracturing of Rock Bodies

Hydraulic fracturing of rock is a complex process involving the interaction of high-pressure fluids with solids, as well as leading to rock rupture and fracture expansion. In this process, the fracture initiation, extension and extension are affected by a variety of factors, and in this section, the rupture, extension and extension of hydraulic fractures in the rock will be explored and investigated in terms of the aperture size, and the ground stress conditions in which the rock body is located.

#### 3.1 Impact of Geostress Conditions on Hydraulic Fracturing

Ground stress, as a natural stress inherent in the formation, has a significant influence on the behavior of hydraulic fracturing cracks. So, numerical simulations to investigate the effects of different stress ratios and stress magnitudes on hydraulic fracturing are very important for hydraulic fracturing design. In this section, hydraulic fracturing simulation tests will be carried out using the rock model described in the previous section in order to investigate the effects of stress ratio, stress magnitude, etc. on the extension and distribution of hydraulic fractures, and the stress condition parameters are shown in Table 2. In the table,  $k$  is  $\sigma_V/\sigma_H$ . Among them, Scenarios 1-5 study the effects of different ground stress ratios on hydraulic fracturing, while Scenarios 6-8 and Scenario 2 mainly study the effects of different ground stress magnitudes on hydraulic fracturing.

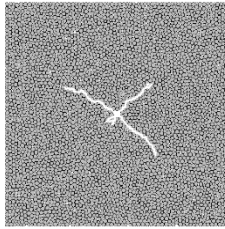
**Table 2.** Calculation scheme for analyzing the effects of stress ratios and ground stress magnitude.

Program numbe	Vertical principal stress $\sigma_V$ (MPa)	Horizontal principal stress $\sigma_H$ (MPa)	Stress ratio ( $k$ )
1	10	10	1
2	20	10	2
3	30	10	3
4	5	10	0.5
5	7.5	10	0.75
6	5	2.5	2
7	10	5	2
8	30	15	2

##### (1) Effect of stress ratio

As shown in Figure 4, the results of crack expansion after loading the five models of Scenarios 1-5 sequentially in Table 2 can be seen from the figure: When the stress ratio  $k$  is less than 1, the direction of crack extension starts along the horizontal direction. And when  $k$  is equal to 1, there is no fixed direction of crack extension, and the three main cracks are basically expanding outward at an angle of  $120^\circ$ ; when the stress ratio

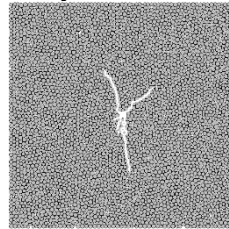
$k$  is greater than 1, the crack basically extends and expands continuously along the vertical direction. It can be seen that the results obtained from the numerical test simulations in this section are consistent with the theoretical analysis.



**Ball**  
**Balls (4458)**  
 ■ ball

**DFN**  
**Fractures (86)**  
 facets

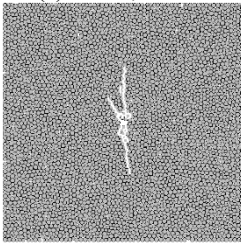
(a)  $\sigma_V=10, \sigma_H=10$



**Ball**  
**Balls (4458)**  
 ■ ball

**DFN**  
**Fractures (85)**  
 facets

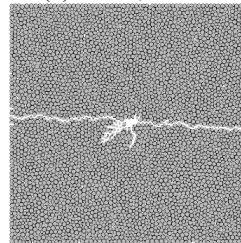
(b)  $\sigma_V=20, \sigma_H=10$



**Ball**  
**Balls (4458)**  
 ■ ball

**DFN**  
**Fractures (84)**  
 facets

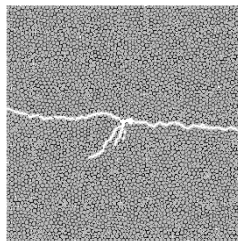
(c)  $\sigma_V=30, \sigma_H=10$



**Ball**  
**Balls (4458)**  
 ■ ball

**DFN**  
**Fractures (167)**  
 facets

(d)  $\sigma_V=5, \sigma_H=10$



**Ball**  
**Balls (4458)**  
 ■ ball

**DFN**  
**Fractures (149)**  
 facets

(e)  $\sigma_V=7.5, \sigma_H=10$

**Fig. 4.** Fracture distribution in the rock mass for different stress ratios.

As shown in Figure 5, the numerical simulation results of the rupture pressure of the rock under different conditions of the ground stress ratio are shown. From the figure, it can be seen that there is a positive correlation between the rupture pressure and the geostress ratio, and the rupture pressure gradually increases with the increase of the geostress ratio  $\sigma_V/\sigma_H$ .

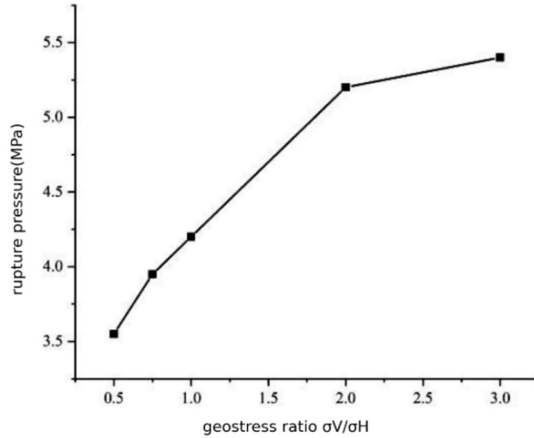
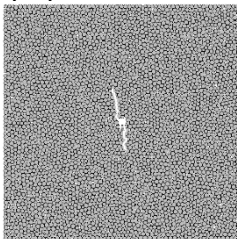


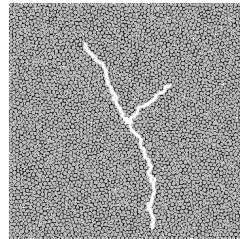
**Fig. 5.** Plot of hydraulic fracturing pressure variation under different ground stress ratio conditions.

(2) Influence of the magnitude of geostress

In order to study the hydraulic crack extension characteristics under different burial depth conditions of the rock body, four ground stress combination schemes are set up in this paper. Among them, the stress ratio  $k$  between vertical and horizontal principal stresses is taken as 2, and the horizontally orientated principal stresses are between 2.5 and 15 MPa. As shown in Fig. 6, the crack extension results after loading under different geostress conditions at the same time for the four rock models of schemes 2, 6, 7 and 8 are shown. From the figure, it can be seen that the magnitude of the ground stress is inversely proportional to the length of the hydraulic cracks.



**Ball**  
**Balls (4458)**  
 ■ ball  
**DFN**  
**Fractures (28)**  
 ■ facets  
 (a)  $\sigma_V=20, \sigma_H=10$



**Ball**  
**Balls (4458)**  
 ■ ball  
**DFN**  
**Fractures (125)**  
 ■ facets  
 (b)  $\sigma_V=5, \sigma_H=2.5$

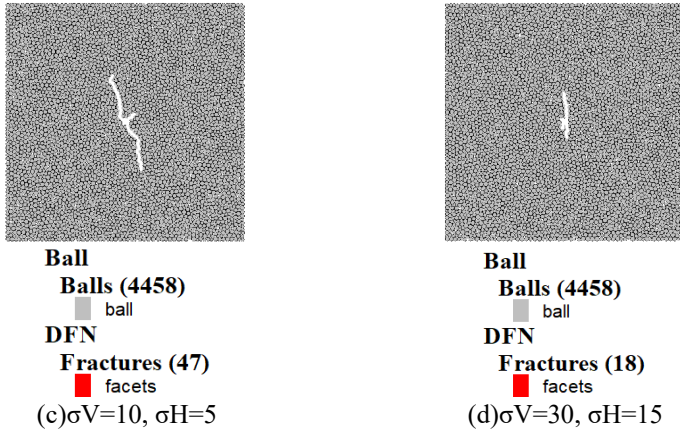


**Fig. 6.** Fracture distribution in the rock mass under different geostress scenarios.

As shown in Figure 7, the curves of the rupture pressure of the rock body under different geostresses, it can be seen from the figure that for rock bodies with higher geostresses, the rupture pressure of the rock body is higher, the more difficult it is to appear hydraulic fracturing phenomenon, and the extensibility of the resulting hydraulic fracture will be poorer. According to the rupture pressure formula for hydraulic fracturing of a homogeneous isotropic intact rock mass proposed by Hubbert and Wills, the higher the ground stress, the higher the rupture pressure required by the rock mass, and thus under the same conditions, the lower the ground stress, the easier it is to rupture the rock mass, and the faster the extension of the fracture will be. From this, it can be seen that the law presented by the experimental simulation results in this section is in line with the traditional hydraulic fracturing theory.

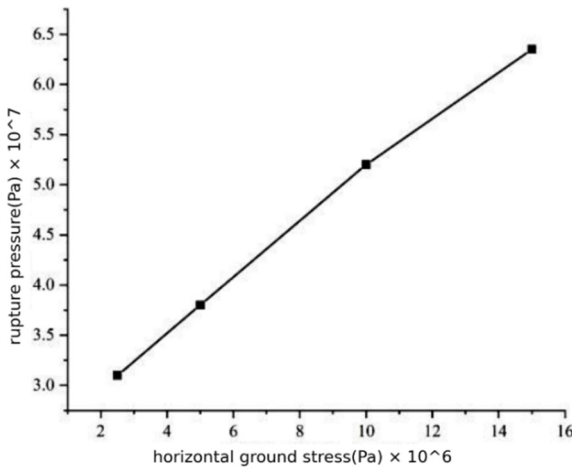


**Fig. 7.** Splitting pressure curves under different geostress magnitude conditions with the same geostress ratio.

### 3.2 Effect of Wellbore Bore Size on Hydraulic Fracturing

Wellbore aperture has an important effect on the fluid flow capacity and area of action, In this section, the effect of wellbore aperture on the behavior of hydraulic fracturing in rocks will be investigated. Five types of borehole diameters were set up, namely 2mm, 5mm, 10mm, 20mm and 30mm, controlling for the consistency of the fine-scale parameters of all five models. At the same time, the ground stress ratio is set to 0.5:1, 1:1 and 2:1, and the transverse principal stress  $\sigma_H$  is constant at 10 MPa. The specific scheme is shown in Table 3.

**Table 3.** Calculation scheme for wellbore bore size impact analysis.

Program number	Stress ratio	Vertical principal stress $\sigma_V$ (MPa)	Horizontal principal stress $\sigma_H$ (MPa)	Hole size (mm)
1	0.5:1	5	10	2
2	0.5:1	5	10	5
3	0.5:1	5	10	10
4	0.5:1	5	10	20
5	0.5:1	5	10	30
6	1:1	10	10	2
7	1:1	10	10	5
8	1:1	10	10	10
9	1:1	10	10	20
10	1:1	10	10	30
11	2:1	10	10	2
12	2:1	10	10	5
13	2:1	10	10	10
14	2:1	10	10	20
15	2:1	10	10	30

The models 11-15 with the ground stress ratio ( $\sigma_V/\sigma_H$ ) of 2:1 was selected for the study. As shown in Figure 8, the direction of expansion is basically along the y-direction, and the longer the length of the cracks appearing in the same time, the fewer the cracks deviating from the y-direction as the wellbore aperture gradually increases from a to e. Cracks with extension directions deviating from the y-direction appear all around the borehole wall of the wellbore in the models, especially in model 11, where the wellbore has a small borehole diameter and appears to be cracked in any direction, this is because there may be uneven stress distribution or material defects around the borehole wall of the wellbore, which can lead to stress concentration around the borehole wall of the wellbore, and cracks can easily develop along the stress concentration points or defects, thus forming cracks.

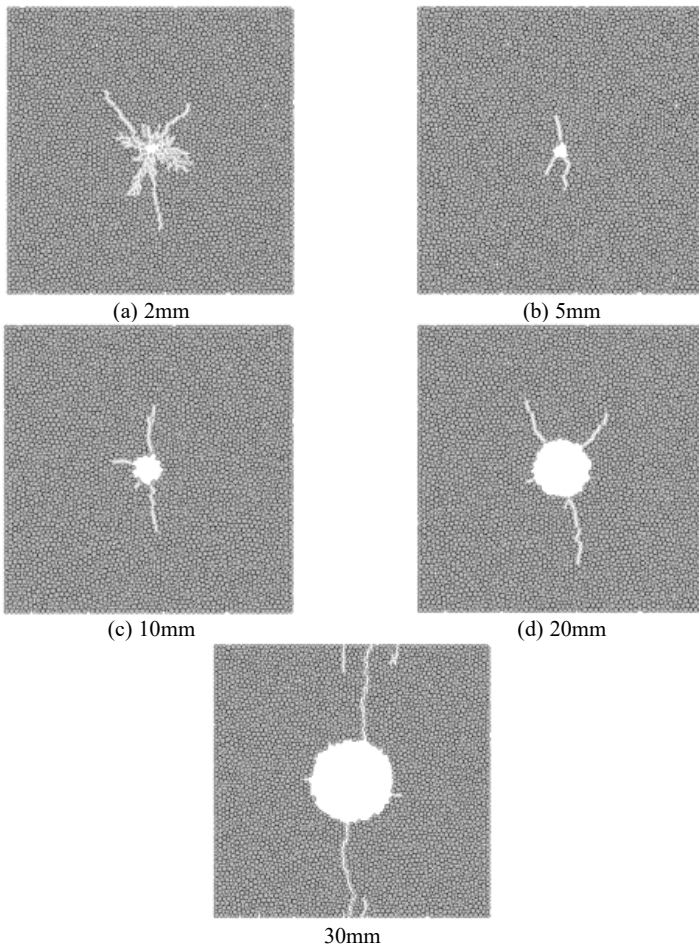


**Fig. 8.** Models 11-15 crack expansion at  $\sigma_V/\sigma_H=2:1$ .

The rupture pressure curves for models 1-15 are shown in Figure 9. From the images, it can be seen that the rupture pressure is inversely correlated with the borehole diameter of the wellbore when the ratio of vertical to horizontal geopressure in the rock envelope is 0.5:1; the rupture pressure decreases with wellbore diameter when the ratio of vertical to horizontal geopressure in the rock envelope is 1:1 versus 2:1, and there is a small increase in rupture pressure at 20 mm diameter, this is due to the increased flow capacity and area of action of the fluid due to the larger pore size, which allows the fracturing fluid to spread over a wider area, resulting in a larger fracture zone and requiring higher pressures; when the ratio of vertical to horizontal geopressure in the rock envelope is 0.5:1 versus 1:1, the rupture pressure is greater for the model with the larger geopressure ratio for the same hole size.

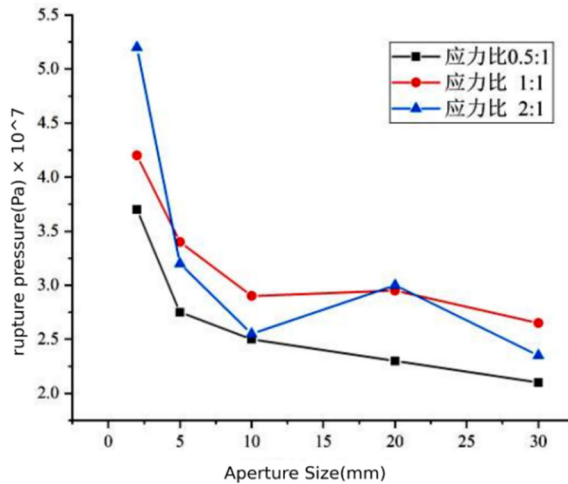


Fig. 9. Models 1-15 rupture pressure profiles.

## 4 Conclusion

In this paper, the hydraulic fracturing simulation algorithm of PFC program is written based on Cundall fluid-solid coupling principle, and the algorithm is verified. The hydraulic fracturing simulation under different influencing factors is carried out to record the pressure change and fracture expansion law. The following results are mainly obtained:

(1) Based on the principle of Cundall fluid-solid coupling, the hydraulic fracturing simulation algorithm of PFC program is written, and the accuracy of the algorithm is verified by comparing the theoretical pressure curves. At the same time, the law of fracture expansion along the direction of maximum principal stress is obtained.

(2) A comparative analysis of the effects of the ground stress ratio and the magnitude of the ground stress on the hydraulic fracturing behavior of rocks revealed that the rupture pressure of hydraulic fracturing of rocks increases with the increase of the ground stress ratio and the ground stress. The cracks tend to extend more vertically when the ground stress ratio increases; the crack length decreases when the ground stress increases.

(3) A comparative analysis of the effect of wellbore borehole diameter on the hydraulic fracturing behavior of the rock by controlling the ground stress ratio reveals that the fracture pressure of the rock gradually decreases as the wellbore diameter increases at a ground stress ratio of 0.5:1; when the ground stress ratios are 1:1 and 2:1, The rupture pressure decreases with wellbore diameter, and there is a small increase in rupture pressure at 20 mm diameter, this is due to the increased flow capacity and area of action of the fluid due to the larger pore size, which allows the fracturing fluid to spread over a wider area, resulting in a larger fracture zone and requiring higher pressures.

## Acknowledgments

This work was financially supported by the National Natural Science Foundation of China (51574296).

## References

1. Heather M. Fracking (2024) Uncertainty: Hydraulic Fracturing and the Provincial Politics of Risk[M]. University of Toronto Press:
2. Song J., Qiao Q., Chen C., et al. (2024) Numerical Analysis of the Stress Shadow Effects in Multistage Hydrofracturing Considering Natural Fracture and Leak-Off Effect[J]. *Water*, 16(9):1308-.
3. Zhang, T., Zheng, Y., Zheng, C., et al. (2022) Study on the influence of fluid injection rate on fracture initiation in shale hydraulic fracturing[J]. *Journal of Hebei University of Engineering (Natural Science Edition)*., 39(04):100-105.
4. Jiang, Y., Wang, Kai., Cai, T., et al. (2024) Study on multi-fracture extension law of hydraulic fracturing with different injection rates[J]. *Coal Engineering*, 56(08):183-189.
5. Huang B., Zhao X., Chen S., et al. (2017) Theory and complete set of techniques for controlling hydraulic fracturing in hard top slabs[J]. *Journal of Rock Mechanics and Engineering*., 36(12):2954-2970.
6. Lin H., Du C. (2011) Experimental study of proposed triaxial hydraulic fracturing in coal rock[J]. *Coal Journal*., 36(11):1801-1805.
7. Tang S., Zhu B., Yan Z. (2011) Effects of geostress on fracture development in hydraulically fractured coalbed methane wells[J]. *Coal Journal*., 36(01):65-69.
8. Papanastasiou P. (1999) An efficient algorithm for propagating fluid-driven fractures[J]. *Computational Mechanics*., 24(4):258-267.
9. Zhang, W., Gao, Y., Liang, L., et al. (2021) Rock mechanical characteristics of conglomerate reservoirs and their impact on fracture modification[J]. *Fractured block oil and gas field*., 28(04):541-545.
10. Li L., Li G., Meng Q., et al. (2013) Numerical simulation analysis of fracture extension pattern of hydraulic fracturing in sandstone[J]. *Geotechnics*., 34(05):1501-1507.
11. Zhang, Y., Zhang, Y., Han, B., et al. (2022) Parameter Studies on Hydraulic Fracturing in Brittle Rocks Based on a Modified Hydromechanical Coupling Model[J]. *Energies*, 15(7):2687-2687.
12. Yang, W., Huang, C., Zhang, Y., et al. (2022) Study on the influence of stress differences on hydraulic fracturing based on true triaxial experiments and discrete element numerical simulations[J]. *Geomechanics and Geophysics for Geo-Energy and Geo-Resources*, 8(5):
13. Yang, W., Li, S., Geng, Y., et al. (2021) Discrete element numerical simulation of two-hole synchronous hydraulic fracturing[J]. *Geomechanics and Geophysics for Geo-Energy and Geo-Resources*, 7(3):
14. Al-Busaidi A, Hazzard J F, Young R P. (2005) Distinct element modeling of hydraulically fractured Lac du Bonnet granite[J]. *Journal of Geophysical Research: Solid Earth*., 110(B6).
15. Lakirouhani A, Detournay E, Bungler A P. (2016) A reassessment of in situ stress determination by hydraulic fracturing[J]. *Geophysical Journal International*., 205(3):

**Open Access** This chapter is licensed under the terms of the Creative Commons Attribution-NonCommercial 4.0 International License (<http://creativecommons.org/licenses/by-nc/4.0/>), which permits any noncommercial use, sharing, adaptation, distribution and reproduction in any medium or format, as long as you give appropriate credit to the original author(s) and the source, provide a link to the Creative Commons license and indicate if changes were made.

The images or other third party material in this chapter are included in the chapter's Creative Commons license, unless indicated otherwise in a credit line to the material. If material is not included in the chapter's Creative Commons license and your intended use is not permitted by statutory regulation or exceeds the permitted use, you will need to obtain permission directly from the copyright holder.

